

Topology changes enable reaction-diffusion to generate forms

Shuhei Miyashita¹ and Satoshi Murata²

¹ Artificial Intelligence Laboratory, Department of Informatics, University of Zurich, Switzerland

`miya@ifi.unizh.ch`

² Interdisciplinary Graduate School of Science and Engineering, Tokyo Institute of Technology, Japan

`murata@dis.titech.ac.jp`

Abstract. This paper demonstrates some examples that show the ability of reaction-diffusion mechanism to code the curvature of forms of multi-cellular systems. The simulation model consists of two layers: the first generates reaction-diffusion waves and the second diffuses chemical substances. The results show that topology changes feedback information to the reaction-diffusion mechanism allowing the control of the morphogenetic process.

Keywords: morphogenesis, reaction-diffusion, geometric topology

1 Introduction

Multicellular organisms usually consist of a large number of cells, which are able to form the shape of an organism by an intricate web of cell-cell interactions, a process called morphogenesis. As each cell contains the same genome, this feat is realized in a distributed and autonomous way with the absence of any centralized control. Although the elucidation of the molecular mechanisms made big progress in biology, an overall picture is still lacking.

In this paper, we hypothesize that morphogenesis depends on the following two conditions:

1. Chemical substances (morphogens) play a role in encoding directly morphological information. In this paper we hypothesize that some substances transmit information by its concentration.
2. Morphogenesis is an autonomous, distributed process without any centralized control for all cells.

We used these two conditions as guidelines to screen the existing literature of morphogenetic models. Alan Turing's reaction-diffusion model [1] uses two chemical substances able to produce spatial patterns in space. As this model uses gradients the first condition is fulfilled, but was not used to form shapes. Essentially reaction-diffusion mechanisms are means of breaking the symmetry among homogenous cells in autonomous and distributed way and therefore

it also fulfills the second condition. L.Wolpert suggested the concept of positional information enabling the cells to know where they are [2]. Gierer and Meinhardt [3] used Turing's model for pattern formations. Murray [4, 5] also presented a possible mechanism for pattern formation in animal markings using reaction-diffusion. Crampin [6] explored the patterns of reaction-diffusion wave accompanied by the extension of space. Kondo [7] pointed out that the change of the stripe pattern in angelfish is driven by reaction-diffusion mechanism. C.Furusawa and K.Kaneko [14] found the phenomena of dynamical cell differentiation by creating their own model. However, all the above examples are mainly focused on pattern generation and not on shape forming. There exist many approaches for morphogenesis - especially in the field of Artificial Life - which can be divided into several types: Lindenmayer grammars [11], cellular automata [12, 18], strictly mechanical approaches where physical interactions between the cells were programmed to simulate morphological processes [10], recurrent diagram networks to express the bodies of simulated creatures [13]. However, the correspondence between these models and real organisms has been considered less seriously. More recently there was renewal of interest in the relations between gene regulatory networks and morphology [15][17][16][19][20], but these models pay little attention to the relation between morphogenesis and reaction-diffusion mechanism. The reason may be that only a few people noticed a possible link between pattern generation and morphological form of creatures. In this paper the linking between reaction-diffusion mechanisms and cell division and physical interactions between the cells can be used to produce shapes of organisms. We focused our research on the change of the geometric topology of cellular networks and found that topology changes can be used to feedback information from the transformed field to the reaction-diffusion mechanism. This feedback made it possible to create a model of the gastro-intestinal tract as an example to show how each homogeneous cell realizes global shapes by computer simulation. The main point of this paper is that the feedback of information of topological changes about the reaction-diffusion mechanism is an essential ingredient to model morphogenetic processes by reaction-diffusion approaches.

This paper is constituted as follows: First biological background is explained, reaction-diffusion system and the developed model are presented in the next section 2. In the third section, the simulation results are shown and the fourth section discusses the results and the conclusions are presented in the last section.

2 Model

In general, multicellular organisms, especially animals, have a gastrointestinal tract, which is essentially a tube from mouth to anus. A cross section of the gastrointestinal tract in humans can be divided into three layers. Going from the inside to outside, the first layer is the epithelium that covers the surface with epithelial cells, connective tissue, and a muscular coat that takes on a role of contraction [8]. Epithelial cells are connected to each other through tight junctions, adhesion belts by cadherins and desmosomes, and gap junctions through which

small molecules can pass. Epithelial cells connect to a matrix below (Extra-Cellular-matrix:ECM) via hemidesmosomes or integrins. For a long time, the ECM had been considered as a physical crutch or anchorage. Recently, however, it became clear that the ECM has more active functions such as passing some specific molecules or controlling the form of a cell that is attached to it. Taking the human gastrointestinal tract as an example, three kinds of curvatures of different scales on epithelium layer can be observed. They are called plicae circulares, villi and microvilli in descending order. This architecture increases the surface area, which facilitates the uptake of food by the gastrointestinal tract. Focusing on this hierarchical form of the epithelial surface, H.Honda advocates that in general the form of multi cellular system is realized as two-dimensional sheets rather than three-dimensional solids [9].

2.1 Two layer reaction-diffusion model

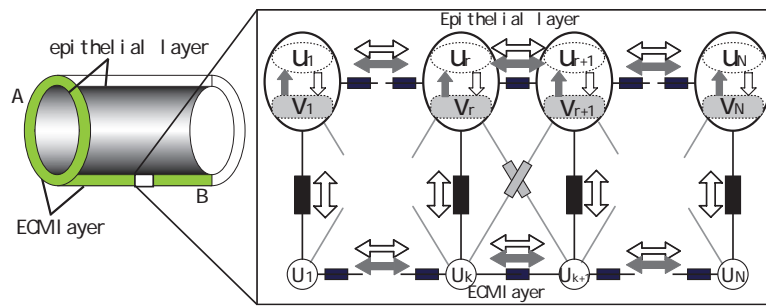


Fig. 1. Two layer model. Upper layer represents epithelial cells and lower layer represents ECM. Epithelial layer can generate reaction-diffusion wave. ECM just diffuses chemical substances.

The cross-section of the gastrointestinal tract can be modeled as two layers for simplification, the epithelial layer and the ECM, which includes submucosal layer and the below. The simulations are performed on a one-dimensional cell array. Fig.1 shows a schema of this model and its correspondence to the biological gastrointestinal tract. Upper nodes represent cells, lower ones represent connection points of each epithelial cells and ECM. Both are expressed as mass points. Links between them are represented as chemical and mechanical connections (chemical substances only diffuse through horizontal and vertical connections, see Fig.1). The mechanical interactions are expressed as spring and damper connections. Epithelial cells contain two chemical substances that react and diffuse, in order to generate reaction-diffusion waves. A reaction-diffusion wave is a periodic spatial concentration pattern (see [1]). The general form of a two chemical reaction-diffusion system can be expressed as partial differential equations (eq.1,2).

$$\dot{u} = f(u, v) + D_u \nabla^2 u \quad (1)$$

$$\dot{v} = g(u, v) + D_v \nabla^2 v \quad (2)$$

$$\begin{aligned} f(u, v) &\equiv +5u - 6v + 1 - \underline{(u-1)^3} \\ &= +2u + 3u^2 - u^3 - 6v + 2 \end{aligned} \quad (3)$$

$$\begin{aligned} g(u, v) &\equiv +6u - 7v + 1 - \underline{(v-1)^3} \\ &= +6u - 10v + 3v^2 - v^3 + 2 \end{aligned} \quad (4)$$

$$\dot{u} = D \nabla^2 u \quad (5)$$

Where u, v represent concentrations of the two chemicals, $f(u, v)$ and $g(u, v)$ represent reaction parts between chemicals u and v , respectively. $\nabla^2 u$ and $\nabla^2 v$ represent the Laplacian of u and v respectively. D_u, D_v and D represent diffusion coefficient of activator, inhibitor and also activator, respectively. Usually a proportion D_v/D_u plays a key role in the behavior of reaction-diffusion system. Since chemical substances diffuse to neighboring cells and the ECM via different channel, it seems reasonable to assume that the diffusion coefficients differ among internal epithelial connections and among epithelial-ECM connections. We set that only the activator can pass through the connection between epithelial cell and ECM. Eq.3,4 is applied for the reaction part, which adds the non-linear term (underlined in eq.3,4) to the Turing's model in order to be more stable fulfilling a definition of activator and inhibitor ($\frac{\partial u}{\partial v} < 0, \frac{\partial v}{\partial u} > 0$). The equilibrium points are the same as Turing's ($u = 1.0, v = 1.0$). The function of the ECM is just to diffuse chemical substances. Its general form can be expressed in eq.5. To the system, Dirichlet boundary conditions were applied, which set the chemical flow at the boundary to zero ($\frac{du_1}{dx} = \frac{du_N}{dx} = 0, \frac{dv_1}{dx} = \frac{dv_N}{dx} = 0, \frac{dU_1}{dx} = \frac{dU_N}{dx} = 0$). Here, $u_1, u_N, v_1, v_N, U_1, U_N$ represent the concentrations of boundary cells and ECM.

2.2 Cell cycle and cell division

Cell cycle is determined by various factors, in this paper, the condition for cell division depends on the concentration and a specific threshold. Cells divide when the concentration of the activator is kept over a specific threshold for a certain time. The concentration of each chemical substance right before division is applied to the concentration of the cell divided.

Fig.2 illustrates the rule controlling how cells reconnect after they divided. Where a represents distance from epithelial cell to ECM and b represents connection length between two cells. Fig.2 a) shows that after cell divides, a new link is added, then an $2\sin(b/2a)$ [rad] angle of curvature is created depending on the ratio of the length of horizontal and vertical links. Since the operating mechanism of the extend speed of ECM hasn't been clear, the ECM's extension speed is assumed to be constant. Fig.2 b) illustrates the correspondence to real tissue after the curvature is created.

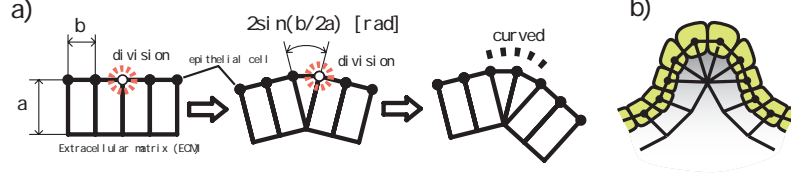


Fig. 2. Reconnection by cell division. a) After each cell divides, a new link is added, then an $2\sin(b/2a)$ [rad] angle of curvature is created depending on the ratio of the length of horizontal and vertical links. b) Correspondence to real tissue.

3 Simulations

$$\begin{aligned} du_r/dt = & +2u_r(t) + 3u_r^2(t) - u_r^3(t) - 6v_r(t) + 2 \\ & + D_{u_{epi}}\{u_{r-1}(t) + u_{r+1}(t) - 2u_r(t)\} + D_{u_{epi-ECM}}(U_k - u_r) \end{aligned} \quad (6)$$

$$\begin{aligned} dv_r/dt = & +6u_r(t) - 10v_r + 3v_r^2(t) - v_r^3(t) + 2 \\ & + D_{v_{epi}}\{v_{r-1}(t) + v_{r+1}(t) - 2v_r(t)\} \end{aligned} \quad (7)$$

$$dU_k/dt = D_{u_{epi-ECM}} \sum_r (u_r - U_k) + D_{u_{ECM}}(U_{k-1} + U_{k+1} - 2U_k) \quad (8)$$

By discretizing the space the eq.6,7 can be obtained from eq.3,4. In the same way, eq.8 can be obtained from eq.5. These equations are used to calculate the dynamics of the chemicals, where, u_r and v_r represents the concentration of activator and inhibitor in epithelium cell, respectively. U_k represents the concentration of activator in ECM. Subscript r and k is an identification number of the cell and the ECM, respectively. The parameters are set as follows: $D_{u_{epi}} = D_{u_{ECM}} = 1.0$, $D_{v_{epi}} = 3.0$, $D_{u_{epi-ECM}} = 0.53$, $u_{threshold} = 1.035$, initial concentration $(u, v) = (1.0, 1.0)$ (equilibrium point). If the concentration exceeds a division threshold for more than 50 steps (step is defined below), a cell divides. Initial perturbations are always added at the center of the epithelial layer.

$$m\ddot{q}_i + c \sum_j (\dot{q}_i - \dot{q}_j) + k \sum_j \left(1 - \frac{l}{|q_i - q_j|}\right) (q_i - q_j) = 0 \quad (9)$$

Cells move on a two-dimensional space. The equation of motion for the cell i is expressed in eq.9 where subscript i, j is an identification number of the cell or connection point to ECM. The position of the cell q_i is defined as a vector. The cell which exists in neighbor of cell i is denoted as j . m, c, k , and l denote mass, damper coefficient, spring coefficient and natural length of spring, respectively. These parameters are set as follows: $m = 9$, $c = 30$, $k = 50$, $l_{hor} = 18$, $l_{ver} = 40$. Every differential equation is integrated by the Euler method ($\delta t = 0.05$, 1step=20 δt). Mechanical forces are calculated assuming in vivo time scales ($\delta t = 0.005$, 1step=60 δt).

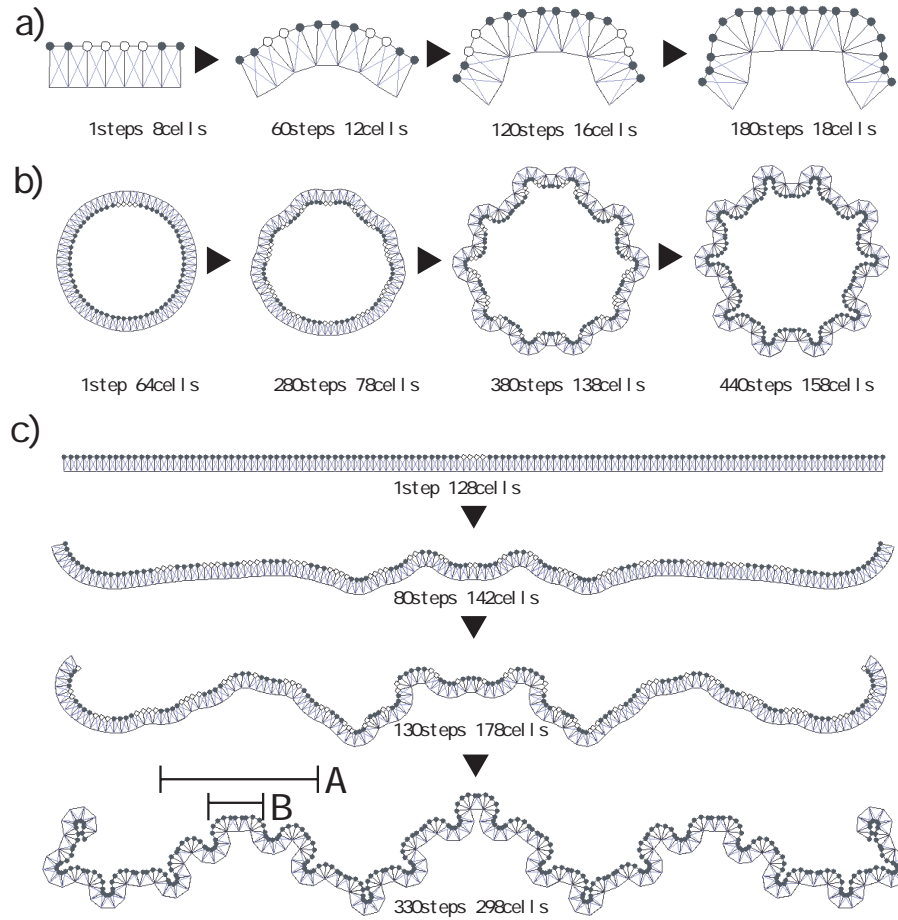


Fig. 3. Simulation results in chronological order. a) Sectional side view of the gastrointestinal tract (Fig.1 B). It can be seen that layers bend by cell division. b) The longitudinal section of the gastrointestinal tract (Fig.1 A). Curvatures are also created independently of the boundary condition. c) Sectional side view of the gastrointestinal tract (Fig.1 B). Unexpectedly, two different curvatures of different scales are formed like Koch-curve. In all results, epithelial cells stop dividing automatically at the end.

Fig.3 a), b), and c) show the simulation results in chronological order. The number of initial epithelial cells are set to 8, 64 and 128, respectively. White colored cells represent those in which the concentrations of activator exceed the threshold. Fig.3 a) shows a sectional side view of the gastrointestinal tract (Fig.1 B). It can be seen that the curvature is created depending on the difference of the extension speed between epithelial layer and ECM. Fig.3 b) shows the longitudinal section of the gastrointestinal tract. The internal layer corresponds

to the epithelial layer and the external layer to the ECM (Fig.1 A). Perturbation is added on the top. Curvatures are also created independently of the boundary condition. Fig.3 c) shows a sectional side view of gastrointestinal tract (Fig.1 B). As time passes, unexpectedly, two different curvatures of different scales are formed on the surface. Finally, fractal hierarchies like Koch-curve are observed (We shall return to this point later). In all results, it can be seen that epithelial cells stop dividing automatically at the end.

Fig.4 a) and b) show the concentration transition of all cells that start at 128 cells. a) and b) show concentration of activator with division threshold and inhibitor, respectively. X-axis represents time and Y represents concentration. As time passes, these concentrations converge and none of the concentrations of activator exceed division threshold after 329 steps. c) and d) show the increase of cell number. The X-axis represents time and Y-axis number of cells in logarithmic scale. (lines pointed by arrows in c) and d) show this model). To quantify the role of the ECM, the diffusion coefficient between the epithelial layer and the ECM changed from 0.0 to 0.8 and plotted on c). The figure shows the smaller the coefficient is, the faster the cell grows. When the diffusion coefficient is 0.8, the number of cells doesn't change, because none of the concentrations of activator exceed threshold. This indicates that the diffusion coefficient between epithelial layer and ECM influences the speed of cell growth. Initial number of cells is changed and plotted in d). It can be seen that the growth mechanism converges independently of the initial number of the cells. The growth rate doesn't change after each transition (around 220% to 250%).

4 Discussions

4.1 The suppression of amplitude of reaction-diffusion wave

Fig.5 shows the maximal amplitude of the activator's concentration generated by the epithelial layer after the number of cells increased from 5 to 11 in different cell topologies (A and B). The X-axis represents the number of cells and the Y-axis the largest concentration. It can be seen that the increase of the curvature suppresses the reaction-diffusion wave. When the number of cells becomes larger than 8, all concentrations of activator become below threshold. This is because the ECM, which connects several cells plays a role of averaging activator that is contained in epithelial cell (Eq.8). Thus as the number of connecting cells increases, concentration of ECM becomes closer to the average of all concentrations that connect (usually $u = 1.0$). Consequently, the reaction-diffusion wave is inhibited. This can also be confirmed by settling all concentration of activator of ECM 1.0 when layers are straight.

Fig.6 shows the growth speed of epithelial cells depending on two parameters: the division threshold and the diffusion coefficient between epithelial layer and ECM. The growth speed is defined as follows: the number of cells at 300 steps / initial number of cells (this time 8). In fig.6 a), X-axis represents diffusion coefficient, y division threshold and z growth speed. In fig.6 b), X-Y plane area is also represented with contours and its forms when the growing speed is 1.5, 2.0,

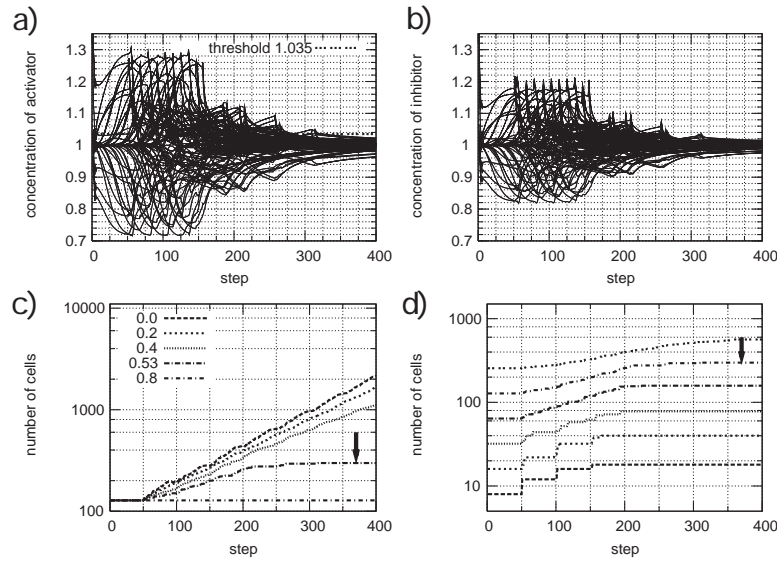


Fig. 4. Transition graph. a) Transition of concentration of activator. b) Inhibitor. These concentrations converge as time passes and no concentration of activator exceeds division threshold after 329 steps. c) d) Increase of the number of cells. c) To quantify the role of the ECM, the diffusion coefficient between the epithelial layer and the ECM is changed from 0.0 to 0.8 and plotted on it. As the figure shows the smaller the coefficient is, the faster the cells grow. d) Only the initial number of cells differs. It is revealed that the mechanism of growth convergence is not dependent on the initial number.

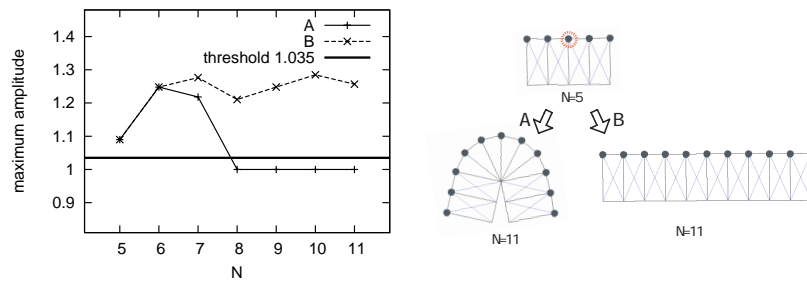


Fig. 5. Maximal amplitude of the activator's concentration. Increase of the curvature suppresses reaction-diffusion wave.

and 2.25. By shifting diffusion coefficient to smaller, the ratio of reaction-parts / diffusion-parts gets larger in their reaction-diffusion system. This makes the amplitude of reaction-diffusion wave bigger: the smaller the diffusion coefficient becomes, the faster growth speed becomes.

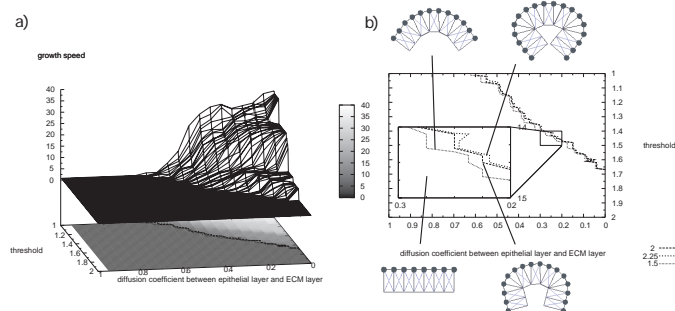


Fig. 6. Growth speed of epithelial cells depending on two parameters. a) The X-axis represents diffusion coefficient, Y represents division threshold and Z represents growth speed. b) X-Y plane area of the same figure. Though it seems these parameters have thin range, note that the curvature depends on the ratio of horizontal-vertical length of the links (see Fig.2).

4.2 Hierarchy of the form

In Fig. 3 c), two different scales of curvatures are formed (A and B). The small curvatures are formed because the epithelial layer and the ECM have different extending speeds. The large scales are created due to mechanical interactions between cells, which extend initial small mechanical perturbations due to cell divisions. This large curvature is always observed, when the layers have a certain length. Each curvature is formed based on their mechanisms and this is the reason why the scales vary. Since friction between gastrointestinal organs and its outer has not been modeled, external forces can erase the large curvature.

5 Conclusions

This paper focused on geometric topology changes of cell networks and shows that topology changes enable reaction-diffusion mechanisms to control morphologic process. In other words, the shape that is driven by reaction-diffusion can build up a feedback loop back to reaction-diffusion mechanism. The model is comprised of two layers: one is the epithelial layer that generates reaction diffusion waves and the other is the ECM that diffuses chemical substances. Cells divide depending on the reaction-diffusion mechanism. Once the shape gets round, chemical substances are averaged at middle point, inhibiting the amplitude of the reaction-diffusion wave. Since the cell division depends on the concentration of activator in this model, it restricts system's growth. This closed feedback loop is one of the autonomous distributed ways to code morphogenesis by supposing that chemical substances act as a transmitters of positional information.

Acknowledgment Many thanks to Peter Eggenberger Hotz for helpful suggestions. This research is supported by the Swiss National Science Foundation, project #200021-105634/1.

References

1. A.M.Turing: A reaction-diffusion model for development, The chemical basis of morphogenesis, Phil Trans. Roy. Soc. of London, Series B; Biological Sciences, **237**, 5, PP.37-72 (1952)
2. L.Wolpert: Positional Information and the Spatial Pattern of Cellular Differentiation, J. Theoret. Biol., **25**, PP.1-47 (1969)
3. A.Giere, H.Meinhardt: A theory of biological pattern formation. Kybernetik, **12**, PP. 30-39 (1972)
4. J.D.Murray: A pattern formation mechanism and its application to mammalian coat markings. In 'Vito Volterra' Symposium on Mathematical Models in Biology, **39**, PP. 360-399 (1979)
5. J.D.Murray: On pattern formation mechanisms for Lepidopteran wing patterns and mammalian coat markings, Phil. Trans. Roy. Soc. of London B, **295**, PP. 473-496 (1981a)
6. E.J.Crampin, E.A.Gaffney, and P.K.Maini: Reaction diffusion on growing domains: scenarios for robust pattern formation, Bull. Mathematical Biology, **61**, PP.1093-1120 (1999)
7. S.Kondo: A reaction-diffusion wave on the skin of the marine angelfish Pomacanthus, Nature, **376**, PP. 765-768 (1995)
8. B.Alberts, A.Johnson, J.Lewis, M.Raff, K.Roberts, P.Walter: Molecular biology of the cell. 4th ed. Garland Science (2002)
9. H.Honda: The mathematical and physical analysis of morphogenesis, Kyoritsu-shuppan (2000)
10. M.Odell, G.Oster, P.Alberch: The Mechanical Basis of Morphogenesis, Developmental Biology **85**, PP.446-462 (1981)
11. A. Lindenmayer: Mathematical Models for Cellular Interaction in Development, Journal of theo-retical Biology, **18**, PP.280-300 (1968)
12. C.G.Langton: Self-reproduction in cellular auto-mata, Physica D: Nonlinear Phenomena, **10**, Issues 1-2, PP.135-144 (1984)
13. K.Sims: Evolving 3d morphology and behavior by competition. Artificial Life, **1**, Issue 4, PP.353-372 (1995)
14. C.Furusawa and K.Kaneko: Emergence of Multicellular Organisms with Dynamic Differentiation and Spatial Pattern, Artificial Life 4 PP.79-93 (1998)
15. P.Eggenberger: Evolving morphologies of simulated 3d organisms based on differential gene expression, Fourth European Conference of Artificial Life, Cambidge, MIT Press (1997).
16. P.Eggenberger: Genome-physics interaction as a new concept to reduce the number of genetic parameters in artificial evolution. Proceedings of the Congress of Evolutionary Computation, Canberra (2004)
17. J.Bongard: Evolving modular genetic regulatory networks. Proceedings of The IEEE 2002 Congress on Evolutionary Computation PP.1872-1877 (2002)
18. K.Tomita, H.Kurokawa, S. Murata: Graph Auto-mata: Natural Expression of Self-reproduction, Physica D: Nonlinear Phenomena, **171** No.4, PP.197-210 (2002).
19. K.Fleischer and A.H.Barr: A simulation testbed for the study of multicellular development : The multiple mechanisms of morphogenesis, Proceedings of the Workshop on Artificial Life, Santafe, NewMexico, PP.389-416 (1994)
20. D.Stork, B.Jackson and S.Walker: Non-Optimality via Pre-adaptation in Simple Neural Systems, Artificial Life II, Addison-Wesley (1992)